Molecular Conformations of Monodendron-Jacketed Polymers by Scanning Force Microscopy

Svetlana A. Prokhorova,[†] Sergei S. Sheiko,*[,†] C.-H. Ahn,[‡] V. Percec,[‡] and Martin Möller*[,†]

Organische Chemie III, Universität Ulm, D-89069 Ulm, Germany, and The W. M. Keck Laboratories for Organic Synthesis, Department of Macromolecular Science, Case Western Reserve University, Cleveland, Ohio 44106-7202

Received August 24, 1998; Revised Manuscript Received January 12, 1999

ABSTRACT: Scanning force microscopy on monodendron-jacketed linear polystyrenes demonstrated unusual conformations and ordering depending on the branching density and interplay between intramolecular and surface interactions of the dendritic coat. Single molecules were visualized as wormlike cylinders, which could be twisted to plectonemic coils or aligned in nematic-like order on the substrate. The attained resolution enabled identification of chain-end stacking, hairpin folds and crossovers of individual macromolecules. The structure of the more densely branched 3,4,5-tris[3′,4′,5′-tris(*n*-dodecan-1-yloxy)benzyloxy]benzyl was predominantly controlled by the intramolecular repulsion of the crowded dendron substituents which enforced an extended conformation of the molecular backbone. Formation of molecular monolayers was affected by wetting/dewetting events during casting, and the film structure did not depend on the substrate type. In contrast, the less crowded 3,4,5-tris[4-(*n*-tetradecan-1-yloxy)-benzyloxy]benzoate (14-ABG-PS) was demonstrated to undergo conformational transitions upon drying and adsorption, as indicated by the observed built-up of torsional stress in the backbone. On mica, 14-ABG-PS formed a web of intertwined twisted cylinders. On graphite, lattice matching between the crystalline surface and the all-trans conformation of the alkyl side chains caused alignment of the macromolecules according to the 3-fold symmetry of highly oriented pyrolytic graphite. Subsequent annealing resulted in the formation of large domains of parallel aligned macromolecules.

Introduction

Precise control of the primary structure and the segmental interaction of natural macromolecules enables them to adopt peculiar tertiary structures, e.g. formation of globules. In contrast, the introduction of secondary bonding in synthetic polymers typically leads to the formation of entangled structures and precipitation. So far, the introduction of dense and multiple branching provides the only synthetic approach toward particulate molecules, which do not interpenetrate each other but interact via their surfaces. Recent synthetic developments include starlike polymers,[1] dendrimers,[2] and arborescent graft polymers.[3] Polymerization of substituted monomers and macromonomers as well as grafting of linear macromolecules can yield wormlike "hairy rod" molecules,[4] polymacromonomer brushes,[5] and monodendron-jacketed chain molecules.[6,7] These three-dimensional (3D) molecules have been discussed as valuable building units for a future nanotechnology as biochemical sensors,[8] molecular containers,[9] and templates for nanolithography.[10]

A question of current interest regards the dependence of the molecular shape on the primary structure, i.e., branching density and topology in combination with nonbonding interactions and the concurrent effects on the intermolecular forces and ordering. One of us has developed new synthetic strategies to manipulate the 3D morphology of individual molecules.[11] Both spherically and cylindrically shaped macromolecules have been prepared by attaching monodendron substituents as side groups to linear polystyrene and polymethacrylate. Such monodendron-jacketed polymers were shown to undergo ordering into a hexagonal columnar (Φ_h) or cubic mesophase.[12,13] It was also found that self-assembly of the monodendrons to a cylindrical structure can induce a disordered helical conformation of the backbone.[13,14]

We have further demonstrated that scanning force microscopy (SFM) provides a means to visualize individual molecules of monodendron jacketed polystyrene and polymethacrylate after they have been adsorbed on mica or graphite.[14] It was shown that the length of the dry molecules was half or equal to that of the fully stretched all-trans planar backbone conformation depending on the bulkiness of the substituents. The apparent shrinkage in length is consistent with a disordered helixlike conformation of the backbone.

A question which we have not explicitly addressed so far regards the interaction of the brushlike molecules with the flat solid substrate. Depending on the steric crowding and the chemical structure of the peripheral groups, the molecular conformation and packing in a monolayer may be affected considerably. Here we report on the surface ordering of cylindrically shaped macromolecules with monodendron side groups differing in their branching density. Solution cast films on mica and highly oriented pyrolytic graphite (HOPG) were studied by scanning force microscopy.

Experimental Section

Materials. Two linear polystyrenes with monodendron side groups were obtained as described elsewhere.[11,15] The polymers differ in the branching structure of the monodendron substituents. In contrast to the polystyrene with 3,4,5-tris[4-(*n*-tetradecan-1-yloxy)benzyloxy]benzoate side groups (14-ABG-PS, Scheme 1), the polystyrene with 3,4,5-tris[3′,4′,5′-tris(*n*-

[†] Universität Ulm.
[‡] Case Western Reserve University.

10.1021/ma981326j CCC: $18.00
Published on Web 03/31/1999

Scheme 1

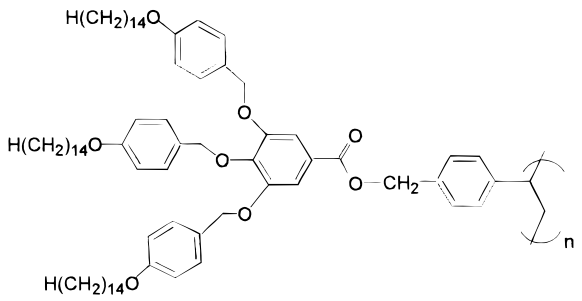

Scheme 2

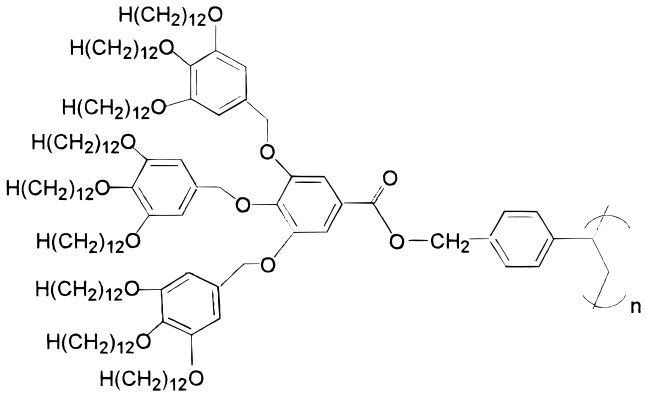

Table 1. Molecular Weight Distribution of 14-ABG-PS and 3,4,5-t-3,4,5-PS As Determined by Size-Exclusion Chromatography and Static Light Scattering

	$\langle M_w \rangle$, kg/mol	$\langle M_n \rangle$, kg/mol	PD
14-ABG-PS			
SEC−PS[a]	280	120	2.4
SEC−UC[b]	1100	400	2.6
SEC-LS[c]	990	470	2.1
SLS[d]	820		
3,4,5-t-3,4,5-PS			
SEC−PS[a]	4000	900	4.4
SEC-LS[b]	2000	900	2.2

[a] Polystyrene calibration. [b] Universal calibration. [c] On-line light scattering. [d] Refractive index increment: $dn/dc = 0.181$ mL/mg.

dodecan-1-yloxy)benzyloxy]benzyl ether side groups (3,4,5-t-3,4,5-PS, Scheme 2) contains nine peripheral alkyl chains per monomer unit. Thus, the molecular weight of the monomer unit of 3,4,5-t-3,4,5-PS was almost 2 times larger than that of 14-ABG-PS, i.e., 2140 and 1194 g/mol, respectively.

Table 1 lists molecular weights and molecular weight distributions which were determined by analytical size-exclusion chromatography (SEC). SEC measurements were done by Waters microstyrogel columns (pore size 10^5-10^3 Å) with THF as a solvent using a triple detection system consisting of a differential refractometer (Waters model 410), a differential viscometer (Viscotek model H502, GPC Win software) and a light-scattering detector (DAWN Model F).[14]

Scanning force microscopy was performed with a Nanoscope III (Digital Instruments) operating in the tapping mode at a resonance frequency of ~ 360 kHz and using Si probes with a spring constant of ~ 50 N/m. Tips with an apex radius below 10 nm were selected by means of a special calibration standard.[16] The standard was also used for calibration of the piezo scanner in the nanometer range. Measurements were done in air at 21 °C under "light-tapping" conditions[17] to minimize damage and indentation of the soft polymer samples.

Samples for the SFM experiments were prepared by the spin casting of dilute cyclopentane, cyclohexane, and chloroform solutions with concentration varying from 0.01 to 0.2 mg/mL. The spin coating was done at room temperature at 2000 rpm on highly oriented pyrolytic graphite and mica as substrates. The samples were annealed at 100 °C for 24 h to approach an equilibrium state of the adsorbed films.

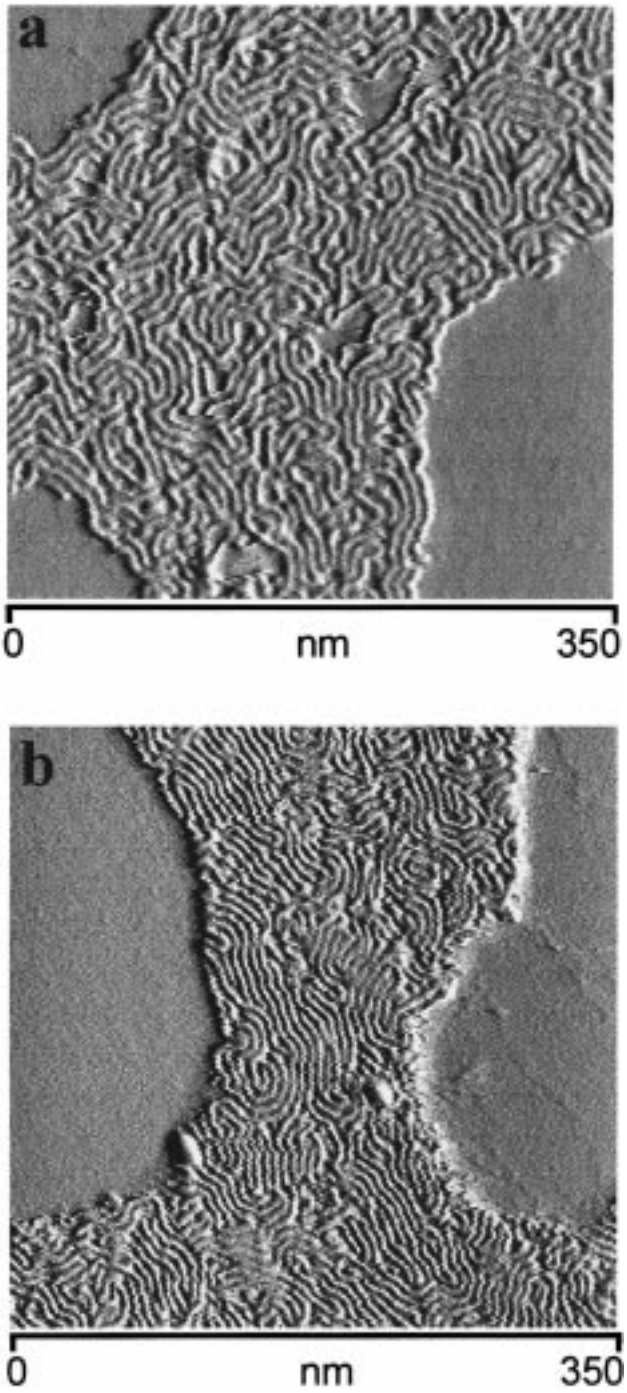

Figure 1. SFM micrographs of 3,4,5-t-3,4,5-PS molecules adsorbed on mica by spin casting from a cyclopentane solution ($c = 0.1$ mg/mL) (a) before and (b) after annealing at 100 °C 24 h. Only within the near range was the parallel alignment of the cylindrical molecules achieved via formation of tight hairpins folds.

Results

1. 3,4,5-t-3,4,5-PS. Figure 1 depicts films of 3,4,5-t-3,4,5-PS polymer on mica before and after annealing. In both cases, the polymer formed a flat monolayer composed of densely packed wormlike molecules. Similar to cylindrical brushes,[5] dense packing was achieved via parallel alignment of the molecules and formation

Table 2. 3,4,5-t-3,4,5-PS on Mica Spincast from Cyclopentane, Chloroform, and Cyclohexane[a]

	before annealing			after annealing		
c, mg/mL	*d*, nm	*h*, nm	*L*, nm	*d*, nm	*h*, nm	*L*, nm
cyclopentane						
0.15	4.8 ± 0.2	3.8 ± 0.2	15−40			
chloroform						
0.3	5.1 ± 0.1	3.6 ± 0.2		5.0 ± 0.1	3.9 ± 0.1	
0.2	4.9 ± 0.2	3.5 ± 0.2				
0.02	5.0 ± 0.1	3.4 ± 0.2				
cyclohexane						
0.25	5.4 ± 0.2	2.6 ± 0.2	20−50	4.6 ± 0.2	2.8 ± 0.3	50−100
0.15	5.2 ± 0.2	2.8 ± 0.1	20−50	4.8 ± 0.1	3.3 ± 0.1	50−100

[a] Key: *d*, intermolecular distance within close packed monolayer; *h*, thickness of the monolayer; and *L*, average length of the straight segment.

Table 3. 14-ABG-PS on Mica Spincast from Cyclopentane, Chloroform, and Cyclohexane[a]

	before annealing			after annealing[c]		
c, mg/mL	*d*, nm	*h*, nm	*L*, nm	*d*, nm	*h*, nm	*L*, nm
cyclopentane						
0.1	5.0 ± 0.1	1.2 ± 0.2	15−30	5.0 ± 0.1	1.9 ± 0.1	15−40
chloroform						
1.0	5.1 ± 0.1	3.5 ± 0.5[b]				
0.7	5.1 ± 0.1	3.5 ± 0.5[b]				
0.3	5.1 ± 0.1	1.8 ± 0.2		5.0 ± 0.1	2.0 ± 0.2	
0.1	5.1 ± 0.1	1.6 ± 0.2				
0.05	5.1 ± 0.1	1.8 ± 0.2				
0.02	5.1 ± 0.1	1.9 ± 0.1				
cyclohexane						
0.25	5.0 ± 0.2	1.6 ± 0.2	10−20	4.9 ± 0.2	1.8 ± 0.2	15−50
0.15	5.0 ± 0.1	1.6 ± 0.1	10−20	4.9 ± 0.2	1.8 ± 0.2	15−50

[a] Key: *d*, intermolecular distance within close packed monolayer; *h*, thickness of the monolayer; *L*, average length of the straight segment. [b] Thickness of the second layer. [c] At 105 °C and 24 h.

of tight hairpin folds. The cross section of 3,4,5-t-3,4,5-PS molecules was fairly circular. The monolayer thickness $h_1 = 3.6 \pm 0.2$ nm and the lateral diameter $d = 5$ nm are in general agreement with the columnar spacing $a = 4.8$ nm from the X-ray diffraction measurements in the mesophase state.[11] The apparent flattening is explained by the squeezing of the material between the tip and the substrate.

Annealing at 100 °C favored formation of larger domains of parallel aligned molecules (Figure 1b), but the distance between molecules remained unchanged. The molecules became more extended so that the maximum length of straight segments increased almost by a factor of 2 from ca. 50 to 100 nm. The monolayer thickness and the diameter of the molecules are presented in Table 2. The slight increase in thickness indicates a tendency to approach a circular cross section.

Similar structures were observed upon adsorption of 3,4,5-t-3,4,5-PS on HOPG (Figure 2a). Films on graphite were uniform in height, and in the near range, the molecules aligned parallel to each other. The ellipsoidal cross section of molecules, which was characterized by 5.2 and 2.5 nm for the larger and smaller diameters, respectively, appeared to be more ablated compared to the same molecules on mica. The deviation from the cylindrical shape might be caused by some energetically favorable alignment of the alkyl chains parallel to the graphite surface. Annealing did not change the monolayer structure considerably (Figure 2b).

To summarize, polystyrene with densely branched monodendron substituents displayed an adsorption behavior similar to other cylindrical molecular objects such as tobacco mosaic viruses,[18] DNA,[19] and "bottlebrushes".[20] The film formation was mainly controlled by adsorption and capillary forces arising during the evaporation process.[21]

2. 14-ABG-PS. Very different behavior was demonstrated for the more loosely branched 14-ABG-PS. Figure 3 shows SFM height micrographs of 14-ABG-PS molecules adsorbed on mica from a cyclopentane solution. Figure 3a depicts a thin film which contains holes of uncovered mica. The diameter of the molecules parallel to the surface plane has been measured to be 5.0 ± 0.1 nm, which is in fair agreement with the column diameter $a = 5.2$ nm from X-ray diffraction in the columnar mesophase state.[11] The thickness of the polymer layer was $h_1 = 1.8 \pm 0.1$ nm, which is considerably smaller than the X-ray spacing $d = 5.4$ nm between the molecules in the columnar mesophase.[12]

The height was measured relative to the hard substrate. As discussed above for 3,4,5-t-3,4,5-PS, the SFM height values might be underestimated because of the surface deformation caused by the tapping tip. In addition to the tip indentation, the smaller value reported here indicates a rather strong interaction with the substrate causing deformation of the molecular cross section. Measurements of the second layer relative to the monolayer surface yielded a thickness of $h_2 = 3.8 \pm 0.2$ nm, which is more consistent with a cylindrical shape of the molecules. Table 3 lists the experimental values of the diameter, the height, and the average length of the straight segments. Within experimental error, the values did not depend on the surface coverage, i.e., casting concentration or solvent.

The enlarged image of the film structure (Figure 3b) shows individual wormlike molecules which cross each other and form an irregular feltlike structure. A cause for the formation of the molecular crossings has been identified by taking a close look at individual molecules at the edge of the film in Figure 4. Some of the protruding wormlike molecules are folded backward and twisted into a superhelix. This peculiar morphology has

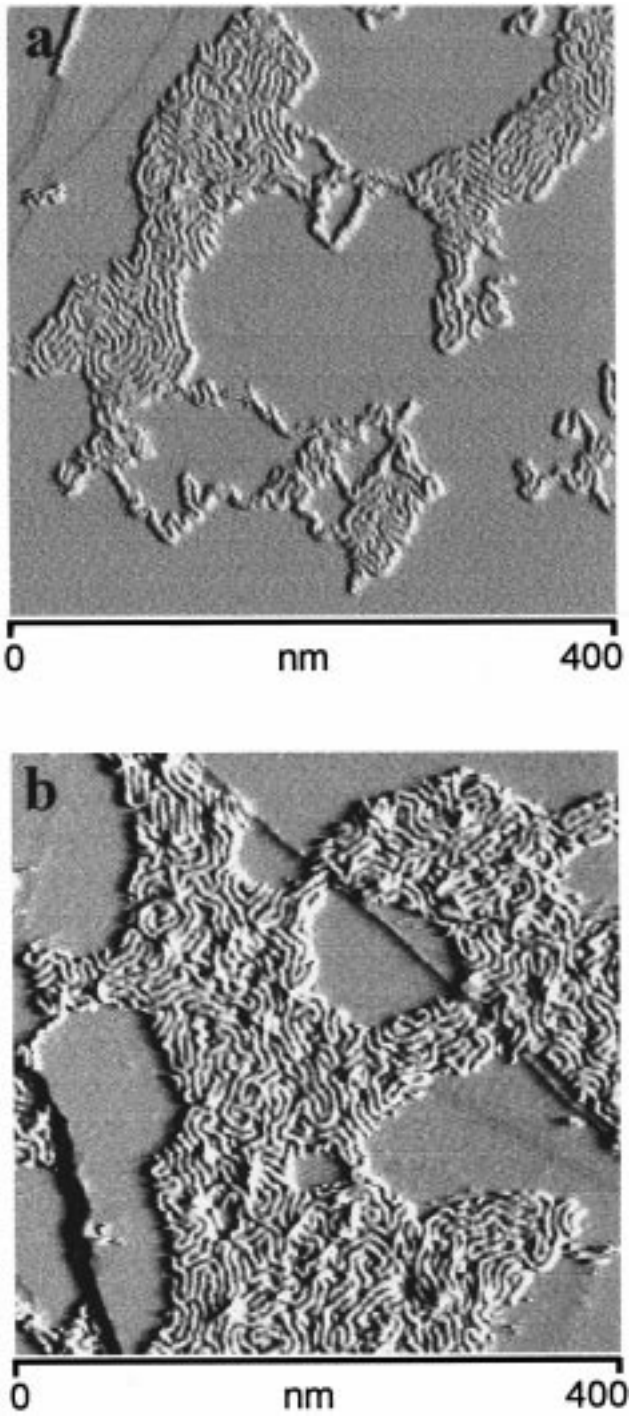

Figure 2. SFM micrographs of 3,4,5-t-3,4,5-PS adsorbed on graphite from cyclopentane solutions ($c = 0.1$ mg/mL) (a) before and (b) after annealing at 100 °C for 24 h.

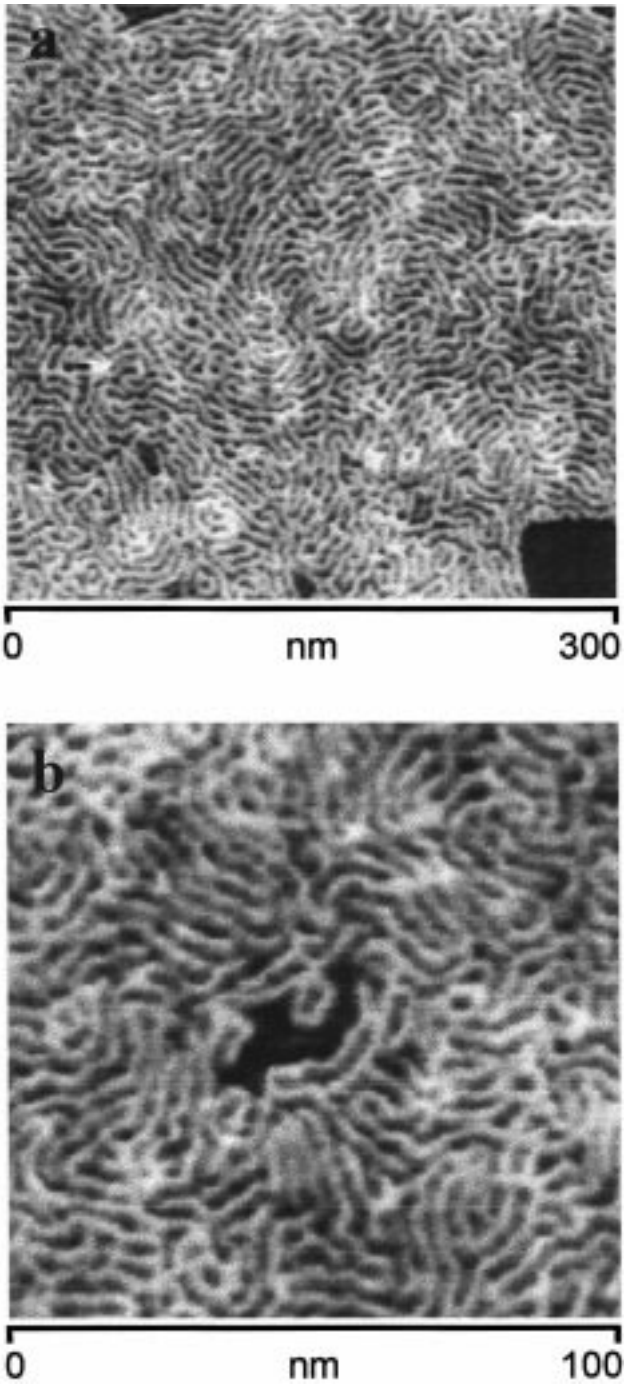

Figure 3. SFM micrographs of a monolayer of 14-ABG-PS prepared by spin casting of 0.1 mg/mL solution in cyclopentane on mica. The wormlike molecules wound around each other and resulted in a feltlike structure.

been verified by a 3D image analysis and cross-sectional profile measurements at the intersection points.

Formation of a superhelix is consistent with a twisted molecular backbone, as is indicated by the longitudinal shrinkage of the 14-ABG-PS molecules.[14] Upon fast evaporation of the solvent, some torsional stress in the backbone can be conserved and drive the molecules to wind around each other and thus release the stress. In this case, the winding direction should be opposite to the molecular torsion, similar to the case of the so-called plectoneme supercoils (from the Greek meaning "braided string")[22,23] which have been described for helical biomolecules.[24−27]

Upon annealing at 60° (Figure 5a) and 105 °C (Figure 5b), the weblike structure vanished. The number of the molecules crossovers decreased, and the segments of the wormlike molecules became arranged more and more in a parallel orientation. The average length of the straight segments (Table 3) became somewhat larger compared to the stressed state. The molecules became untwisted and formed conventional hairpins[28] in place of the plectoneme folds (Figure 5b). Obviously, the stress was released as the bulk isotropization temperature T_i = 103 °C was approached. In addition, the diameter decreased and the height of the molecules increased by about 10% of the original values, approaching a circular geometry.

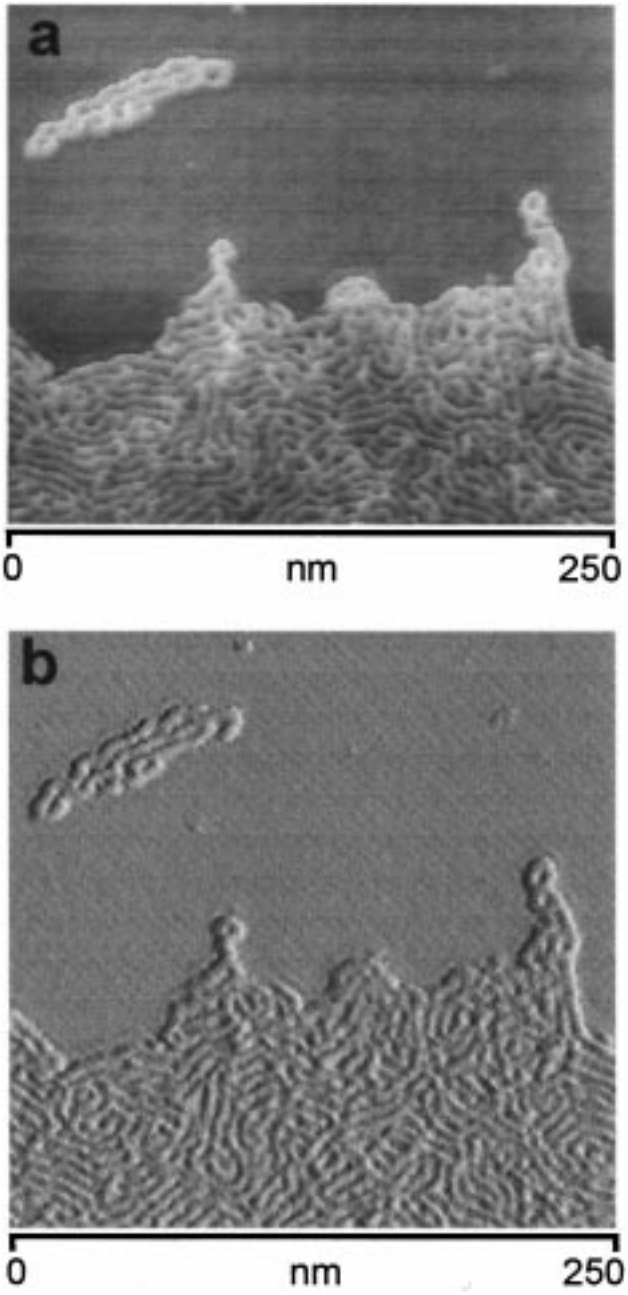

Figure 4. High-resolution (a) height and (b) amplitude SFM micrographs of 14-ABG-PS on mica. Protruding molecules at the film edge (marked by arrows) clearly show the plectoneme conformation caused by the backward folding of the torsionally stressed molecules.

Another unusual morphology of the monodendron-jacketed polystyrene was observed when HOPG was used as a substrate. Parts a and b of Figure 6 show two SFM micrographs of monolayer films cast on graphite at concentrations of 0.1 and 0.06 mg/mL, respectively. Individual molecules of 14-ABG-PS were clearly resolved and displayed a strictly defined orientation with respect to the substrate with characteristic angles of 60° and 120°. This peculiar orientation was observed irrespective of the degree of the substrate coverage, which was ca. 80% in Figure 6a and about 40% in Figure 6b.

The fact that the molecular contour followed the 3-fold symmetry of the graphite might be explained by a specific interaction such as the adsorption of the alkyl side-chains on the HOPG surface.[29−31] Additional evidence for the specific interaction was obtained by

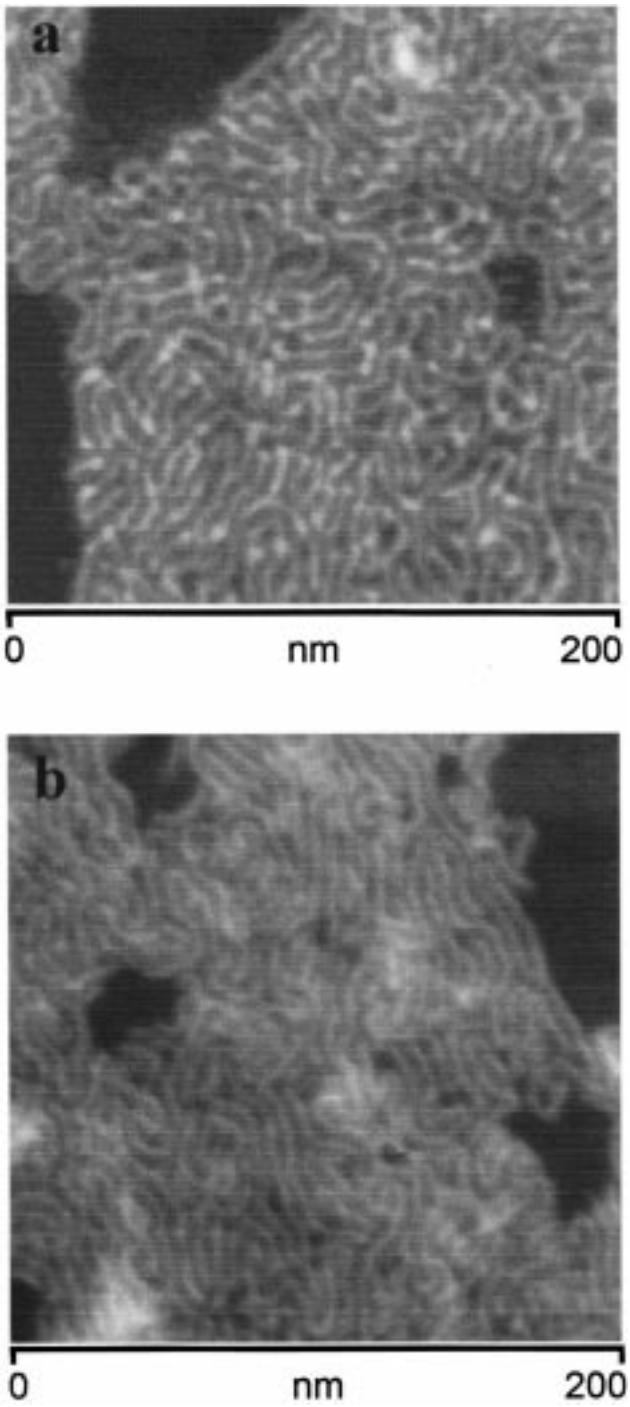

Figure 5. SFM micrographs of the thin film of 14-ABG-PS annealed at (a) 60 and (b) 105 °C for 24 h on mica. Still crossing each other, molecules form conventional hairpins in place of the plectoneme.

increasing the solution concentration above the monolayer coverage. As molecules in the second layer lost direct contact with HOPG, they formed plectoneme coils similar to those on the mica substrate.[22,23] One of these twisted molecules adsorbed onto the monolayer surface is depicted in Figure 6a and marked by the arrow.

Table 4 lists the intermolecular distances, *d*, within close packed domains of 14-ABG-PS on graphite, the height of the monolayer, *h*, and the average length of a straight segment, *L*. The intermolecular distance was well-defined but considerably larger than the X-ray spacing for the columnar mesophase. Furthermore, depending on the substrate coverage, the distance

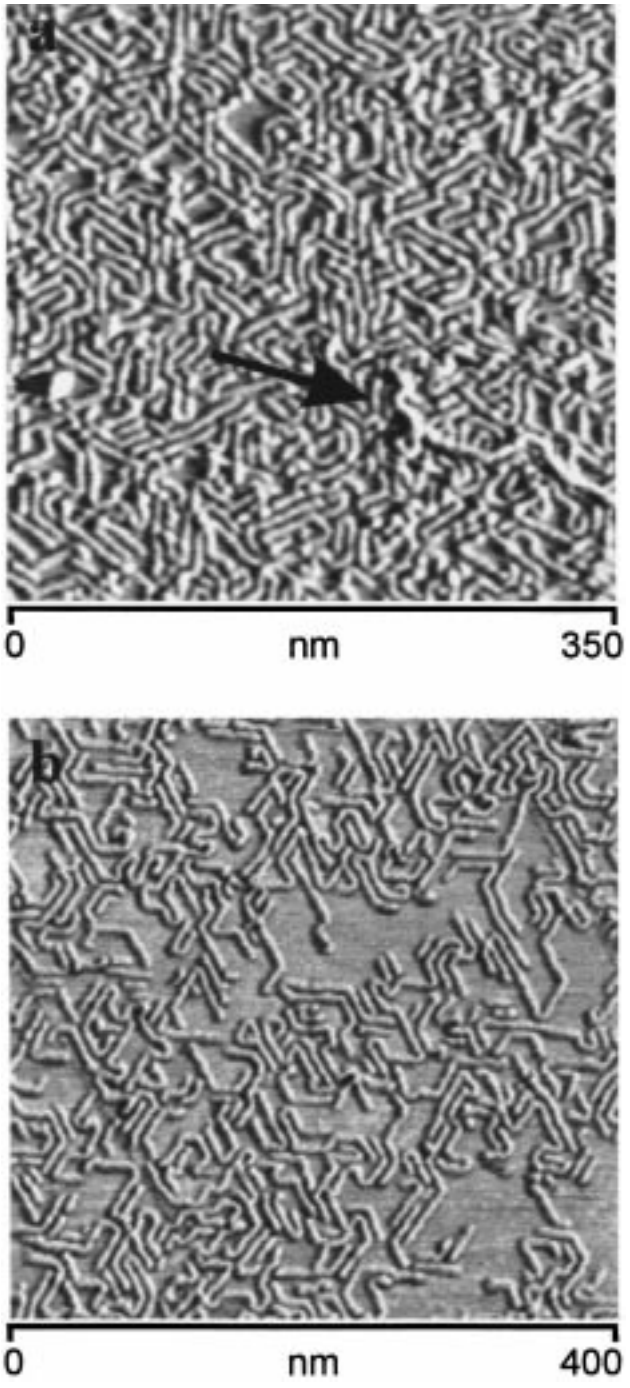

Figure 6. SFM micrographs of the monolayers on HOPG prepared by spin casting of 14-ABG-PS solutions in cyclopentane of different concentrations: (a) 0.1 and (b) 0.06 mg/mL. The higher concentration resulted in a closed monolayer, whereas the more dilute solution yielded individual molecules. In both cases, the molecules aligned parallel to the substrate and bent at characteristic angles of 60° and 120° to follow the 3-fold symmetry of graphite. The arrow in part a shows a wormlike molecule adsorbed onto the monolayer surface which adopts a plectoneme conformation similar to those on mica (Figure 4).

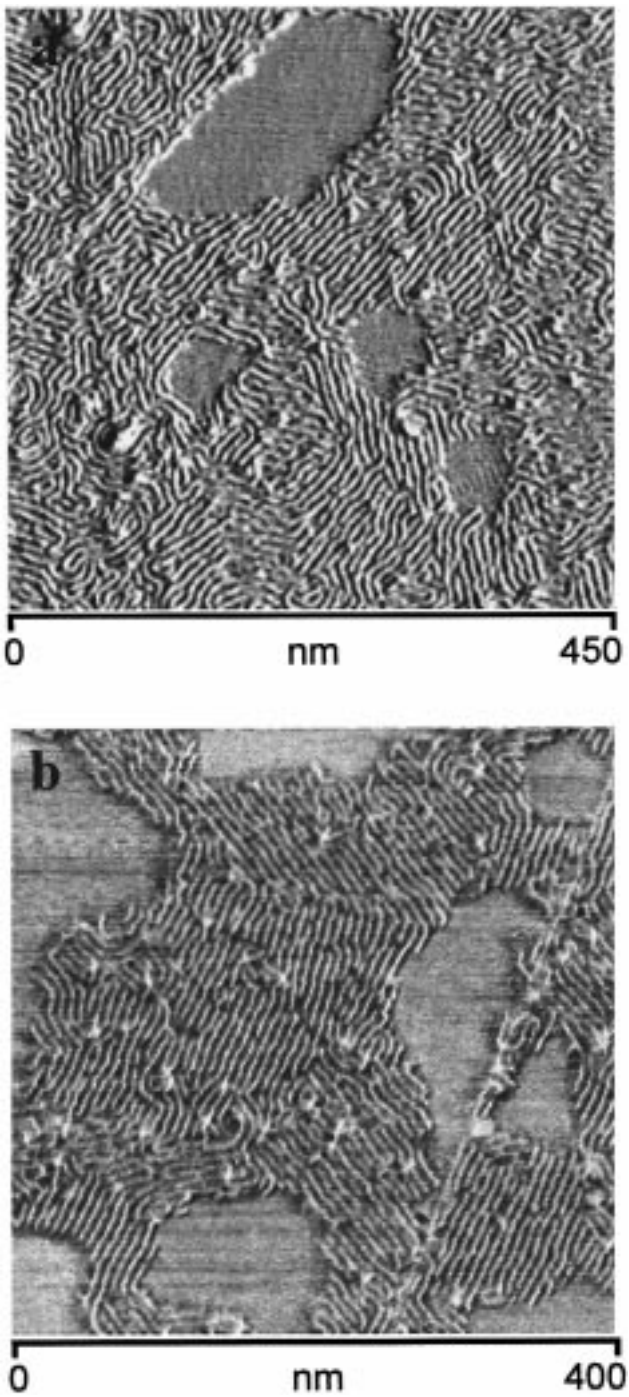

Figure 7. SFM micrographs of the 14-ABG-PS monolayer films shown in Figure 6, after annealing at 100 °C for 24 h. Large domains where the molecules aligned parallel at a defined distance to each other were formed.

varied from 5.8 nm in a close-packed monolayer (c = 0.15 mg/mL) to 8 nm in the monolayer islands (c = 0.01 mg/mL). The larger value is 2-fold of the maximum length of the side chains, which was estimated by a force-field simulation to be 4.4 nm. This indicates that the alkyl side chains stretched almost completely to maximize the coverage of the high-surface-energy substrate by the polymer film. The minimum intermolecular distance of 5.8 nm approaches the spacing of the molecular columns in the mesophase state a = 5.2 nm.

Upon annealing at 100 °C, perfection of the molecular packing occurred. Figure 7 shows micrographs of the same samples depicted in Figure 6 after annealing. The small islands and isolated molecules aggregated into larger domains, and the molecular cylinders aligned nearly parallel to each other. Within the domains, the molecules were completely extended. The average domain size along the axis of the molecules of ca. 200 nm exceeded by far the average length of the individual molecules L_w = 120 nm determined directly from SFM micrographs.[14] The intermolecular distance decreased,

Table 4. 14-ABG-PS on Graphite Spincast at 2000 rpm from Cyclopentane, Chloroform, and Cyclohexane

	before annealing			after annealing		
c, g/mL	*d*, nm	*h*, nm	*L*, nm	*d*, nm	*h*, nm	*L*, nm
cyclopentane						
0.15	5.8 ± 0.2	1.2 ± 0.1	20−50	5.8 ± 0.2	1.2 ± 0.1	20−150
0.1	6.3 ± 0.2	1.1 ± 0.1	15−50	5.8 ± 0.2	1.1 ± 0.2	30−150
0.08	6.5 ± 0.2	1.1 ± 0.2	25−50	6.0 ± 0.1	1.2 ± 0.1	40−100
0.06	7.6 ± 0.2	1.2 ± 0.1	25−50	6.7 ± 0.2	1.3 ± 0.1	25−150
0.05	8.0 ± 0.1	1.3 ± 0.1	20−70	7.3 ± 0.2	1.2 ± 0.1	30−150
0.03	8.0 ± 0.1	1.3 ± 0.1	25−60	7.2 ± 0.2	1.2 ± 0.2	20−150
0.01	8.0 ± 0.1	1.3 ± 0.1	25−50	7.3 ± 0.1	1.2 ± 0.1	25−150
chloroform						
0.2	5.8 ± 0.2	1.3 ± 0.2	25−40	5.3 ± 0.2	1.4 ± 0.2	40−100
0.1	5.5 ± 0.1	1.2 ± 0.2	25−40	5.5 ± 0.1	1.8 ± 0.2	30−100
cyclohexane						
0.15	5.3 ± 0.1	1.6 ± 0.2 3.4 ± 0.3[a]	25−50	5.6 ± 0.1	1.9 ± 0.1	30−100

[a] Thickness of the second layer.

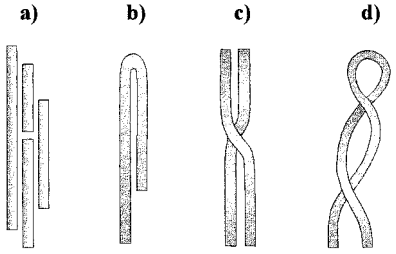

Figure 8. Typical packing defects of 14-ABG-PS molecules adsorbed onto graphite and mica: (a) head-to-end, (b) hairpin, (c) intersections, and (d) plectoneme.

approaching the column diameter in the bulk mesophase state (Table 4). However, the molecules remained significantly flattened by the interaction with the substrate.

Because translational motions of the molecules are confined in two dimensions, a higher degree of orientational order might be expected for a lower substrate coverage. Accordingly, the domain size in Figure 7b was about 2 times larger than that in Figure 7a, where the substrate was coated by approximately 2 times more molecules per unit area. In addition, after annealing, the orientation of the molecules and the domain boundaries are controlled by the 3-fold symmetry of the HOPG surface.

The SFM measurements enabled clear visualization of the chain ends which allowed us to characterize the monolayer structure on a scale of single molecules. Some typical defects, which are inherent for the nonannealed and annealed samples, are sketched in Figure 8. Defects such as (a) chain-end stacking, (b) hairpins, and (c) intersections are typical for the linear polymers. The plectoneme (d) was a peculiar case which was caused by twisting of the monodendron side groups along the helix axis and the concurrent folding of the backbone.

Conclusion

It has been demonstrated that the thick, monodendron-substituted polystyrenes can form well-ordered 2D layers by simple spin-coating procedures. The type of the substrate did not play a significant role in film formation of 3,4,5-t-3,4,5-PS with the densely branched side chains. These macromolecules can be consider as "smooth" cylinders whose surface functionalities are not accessible for specific interactions with the HOPG substrate. 3,4,5-t-3,4,5-PS formed a close monolayer, where the wormlike molecules displayed only near-range orientational order. Film formation was controlled primarily by capillary forces during evaporation of the solvent.

In contrast, the conformation and film structure of the less densely substituted 14-ABG-PS was strongly affected by the interplay of intramolecular and surface forces. When the interaction of the molecules with the substrate was small, i.e., on mica, film formation and the molecular structure of the molecules were strongly affected by the intramolecular forces. This is demonstrated by the plectoneme supercoils resulting in the feltlike film structure of 14-ABG-PS molecules on mica. Supercoiling indicates the built up of torsional stresses as the solvent evaporates and the originally solvated molecular conformation contracts into itself. Obviously, quick evaporation of the solvent resulted in a residual torsion in the adsorbed molecule, which can be due to either underwinding or overwinding of the backbone. Eventually, annealing offered a path for stress relaxation and allowed structural defects to heal.

The supercoiling is consistent with the longitudinal contraction of 14-ABG-PS as it might be expected from the observation of a contour length only half the value of the fully stretched backbone and which was ascribed to a random helix conformation caused by the self-assembly of the tapered side groups into a cylindrical shape.[14] Supercoiling was well-described both experimentally and theoretically for circular DNA[22−26] and even observed for synthetic structures, which might experience the torsion type deformation.[27]

On graphite, the conformation and the monolayer arrangement of the 14-ABG-PS molecules were strongly affected by the specific interaction of the peripheral alkyl chains with the HOPG substrate. In contrast to mica, the wormlike molecules on graphite demonstrated well-defined orientation and long-range positional order. Similar to the well-known adsorption of alkanes, the orientation followed the 3-fold symmetry of the graphite surface.[29−31]

Not only the orientation of the backbone, but also interchain spacing within a packed monolayer, was controlled by the side chains. Depending on the surface concentration of the molecules, the distance between the polymer backbones could be varied from 5.8 to 8 nm. The lower value corresponds to the column diameter in the mesophase state, and the higher distance is given by the contour length of the alkyl side chains.

Finally, the flexible structure in combination with the specific interaction of the 14-ABG-PS favored thermo-

tropic ordering on the graphite surface. Thermal annealing enabled the ordering of molecules over a range exceeding the size of the molecules.

Acknowledgment. This work was financially supported by the Deutsche Forschungsgemeinschaft (Project SH 46/2-1) and Graduiertenkolleg "Molekulare Organization und Dynamik an Ober- und Grenzflächen", NSF (DMR-97−08581) and a Humbolt Research Award for senior U.S. scientists to V.P.

References and Notes

(1) Roovers, J. *J. Non.-Cryst. Solids* **1991**, *793*, 131.
(2) Dvornic, P. R.; Tomalia, D. A. *Curr. Opin. Colloid Interface Sci.* **1996**, *1*, 221.
(3) Gauthier, M.; Möller, M. *Macromolecules* **1991**, *24*, 4548.
(4) Wu, J.; Lieser, G.; Wegner, G. *Adv. Mater.* **1996**, *8*, 151.
(5) Sheiko, S. S.; Gerle, M.; Fischer, K.; Schmidt, M.; Möller, M. *Langmuir* **1997**, *20*, 5368.
(6) Percec, V.; Ahn, C.-H.; Ungar, G.; Yeardley, D. S. P.; Möller, M.; Sheiko, S. S. *Nature* **1998**, *391*, 161.
(7) Karakaya, B.; Claussen, W.; Gessier, K.; Säanger, W.; Schlüter, A.-D. *J. Am. Chem. Soc.* **1997**, *119*, 3296.
(8) Zimmerman, S. C. *Curr. Opin. in Colloid Interface Sci.* **1997**, *2*, 89.
(9) Jansen, J. F. G. A.; de Brabander-van den Berg, E. M. M.; Meijer, E. W. *J. Am. Chem. Soc.* **1995**, *117*, 4417.
(10) Park, M.; Harrison, C.; Chaikin, P. M.; Register, R. A.; Adamson, D. H. *Science* **1997**, *276*, 1401.
(11) Percec, V.; Ahn, C.-H.; Cho, W.-D.; Jamieson, A. M.; Kim, J.; Leman, T.; Schmidt, M.; Gerle, M.; Möller, M.; Prokhorova, S. A.; Sheiko, S. S.; Cheng, S. Z. D.; Zhang, A.; Ungar, G.; Yeardley, D. J. P. *J. Am. Chem. Soc.* **1998**, *120*, 8619.
(12) Hudson, S. D.; Jung, H.-T.; Percec, V.; Cho, W.-D.; Johansson, G.; Ungar, G.; Balagurusamy, V. S. K *Science* **1997**, *278*, 449.
(13) Kwon, Y. K.; Chvalun, S.; Scheider, A.-I.; Blackwell, S.; Percec, V.; Heck, J. A. *Macromolecules* **1994**, *27*, 6129.
(14) Prokhorova, S. A.; Sheiko, S. S.; Möller, M.; Ahn, C.-H.; Percec, V. *Macromol. Rapid Commun.* **1998**, *19*, 359.
(15) Percec, V.; Ahn, C.-H.; Barboiu, B. *J. Am. Chem. Soc.* **1997**, *119*, 12978.
(16) Sheiko, S. S.; Möller, M.; Renvekamp, E. M. C. M.; Zandbergen, H. W. *Phys. Rev.* **1993**, *B48*, 5675.
(17) Magonov, S. N.; Elings, V.; Whangbo, M.-H. *Surf. Sci.* **1997**, *375*, L385.
(18) Maeda, H. *Langmuir* **1997**, *13*, 4150.
(19) Hansma, H. G.; Vesenka, J.; Seigerist, C.; Kelderman, G.; Morett, H.; Sinsheimer, R. L.; Eilings, V.; Bustamante, C.; Hansma, P. K. *Science* **1992**, *256*, 1180.
(20) Dziezok, P.; Sheiko, S. S.; Fischer, K.; Schmidt, M.; Möller, M. *Angew. Chem., Int. Ed. Engl.* **1997**, *109*, 2812.
(21) Kralchevsky, P. A.; Nagayama, K. *Langmuir* **1994**, *10*, 23.
(22) Moroz, J. D.; Nelson, P. *Macromolecules* **1998**, *31*, 6333.
(23) Marko, J. F.; Siddia, E. D. *Phys. Rev. E* **1995**, *52*, 2912.
(24) Cozzarelli, N. R. *Science* **1980**, *207*, 953.
(25) Crick, F. H. C. *Proc. Natl. Acad. Sci. U.S.A.* **1976**, *73*, 2639.
(26) Full, F. B. *Proc. Natl. Acad. Sci. U.S.A.* **1971**, *68*, 815.
(27) Strick, T. R.; Allemand, J.-F.; Bensimon, D.; Croquette, V. *Biophys. J.* **1998**, *74*, 2016.
(28) de Gennes, P. G. *Polymer Liquid Crystals*; Ciferri, A., Krigbaum, W. R., Meyer, R. B., Eds.; Academic: New York, 1982.
(29) Rabe, J. P.; Buchholz, S. *Phys. Rev. Lett.* **1991**, *66*, 2096.
(30) Wavkuschewskij, A.; Cantow, H.-J.; Magonov, S. N.; Möller, M.; Liany, W.; Whanbo, M.-H. *Adv. Mater.* **1995**, *5*, 821.
(31) Wittmann, J. C.; Lotz, B. *Prog. Polym. Sci.* **1990**, *15*, 909.

MA981326J